



COVID-19 symptom identification using Deep Learning and hardware emulated systems



Rashini Liyanarachchi ^{a,*}, Janaka Wijekoon ^b, Manujaya Premathilaka ^c,
Samitha Vidhanaarachchi ^c

^a National University of Singapore, Singapore

^b Military Technological College, Muscat, Oman

^c Sri Lanka Institute of Information Technology, Sri Lanka

ARTICLE INFO

Keywords:

Health care
COVID-19
Transfer Learning
Deep Learning
Artificial Intelligence
Thermal imaging
Cough classification
Cough resemblance

ABSTRACT

The COVID-19 pandemic disrupted regular global activities in every possible way. This pandemic, caused by the transmission of the infectious Coronavirus, is characterized by main symptoms such as fever, fatigue, cough, and loss of smell. A current key focus of the scientific community is to develop automated methods that can effectively identify COVID-19 patients and are also adaptable for foreseen future virus outbreaks. To classify COVID-19 suspects, it is required to use contactless automatic measurements of more than one symptom. This study explores the effectiveness of using Deep Learning combined with a hardware-emulated system to identify COVID-19 patients in Sri Lanka based on two main symptoms: cough and shortness of breath. To achieve this, a Convolutional Neural Network (CNN) based on Transfer Learning was employed to analyze and compare the features of a COVID-19 cough with other types of coughs. Real-time video footage was captured using a FLIR C2 thermal camera and a web camera and subsequently processed using OpenCV image processing algorithms. The objective was to detect the nasal cavities in the video frames and measure the breath cycles per minute, thereby identifying instances of shortness of breath. The proposed method was first tested on crowd-sourced datasets (Coswara, Coughvid, ESC-50, and a dataset from Kaggle) obtained online. It was then applied and verified using a dataset obtained from local hospitals in Sri Lanka. The accuracy of the developed methodologies in diagnosing cough resemblance and recognizing shortness of breath was found to be 94% and 95%, respectively.

1. Introduction

COVID-19 is a worldwide pandemic caused by the highly contagious SARS-CoV-2 virus (Organization, 2022b). This was first discovered in Wuhan, China, in December 2019. Hence this disease has had a detrimental effect on nearly every aspect of the global economy and social structure (Nation, 2022). When a person sneezes, speaks, coughs, or breathes, the minuscule droplets discharged from the nose or mouth transmit the virus. This virus has diverse forms that are now spreading over the world (Organization, 2022a).

During the time this study was carried out, numerous variants of this virus were spreading worldwide. Variants of Concern (VOC) and Variants of Interest (VOI) are two classifications for identified variants. The World Health Organization (WHO) classifies the VOC as Alpha, Beta, Gamma, Delta, and Omicron, and it labels the VOI as Eta, Iota, Kappa, Lambda, and Mu (Organization, 2022c). COVID-19 patients have reported a wide range of symptoms. According to for Disease Control and Prevention (2021), the symptoms are the same irrespective

of the varieties. Similarly, for other respiratory virus infections, such as the common cold or influenza, individuals may experience symptoms such as fever, tiredness, cough, loss of taste or smell, nausea, and shortness of breath. These shared symptoms make it crucial to accurately differentiate between respiratory illnesses to determine the specific virus causing the infection. In addition to the number of fatalities, this pandemic has had a significant negative impact on the global economy (Donthu and Gustafsson, 2020).

The negative impact on the global economy led to the closure of several businesses, factories, and other workplaces. Even during the period of this study, many companies were continuing the struggle to recover their footing. Although some businesses adopted the Work from Home (WFH) concept to sustain operations, many more faced challenges due to their operational procedures, making it difficult to adapt to remote work. Consequently, the businesses that could not operate remotely resumed their operations despite the pandemic. This decision inadvertently contributed to the rapid spread of the virus and a significant increase in reported cases. In Sri Lanka, clusters

* Corresponding author.

E-mail address: rashinikavindya@gmail.com (R. Liyanarachchi).

formed within garment factories, organizations, and shopping malls were responsible for over 95% of the reported cases (Covid19.gov.lk, 2021).

Given the timely importance of preventing the spread of this virus and ending the pandemic, a variety of research is being undertaken all over the world in response to the various challenges that have arisen as a result of it Benfante et al. (2021), del Rio et al. (2020) and Chaguza et al. (2022). Hence, not only the scholarly community allocated substantial financial resources and manpower for research and development to curb this ongoing endemic and future endemics, but also Economic giants initiated vaccination programs incurring an average expenditure of USD 7.7 billion for research and development efforts. The objective was to expedite the development of technologies that could effectively combat the endemic.

To this end, this paper also presents a study of a contactless method to analyze cough sounds and shortness of breath using Deep learning (DL) together with a hardware-emulated system to classify COVID-19 suspects in Sri Lanka. DL is an upcoming and powerful technology used to implement foreseeable applications providing a technical flavor to control this deadly disease. Given that DL can be enhanced by incorporating hardware, numerous research has been conducted in the healthcare industry to tackle the COVID-19 outbreak using DL technology.

Similar studies had been carried out for the early identification of COVID-19 patients using DL and hardware-emulated systems. For Eg., the study in Le et al. (2021) proposed an IoT-enabled Depth Wise Separable Convolution Neural Network (DWS-CNN) with Deep Support Vector Machine (DSVM) to diagnose and classify COVID-19. This paper analyzes Chest X-ray images to classify them as binary or multiple-class labels of COVID-19. This classification process involved data acquisition, Gaussian Filtering, feature extraction, and classification. This system has achieved an accuracy of above 98% for both binary and multiple classifications. Similarly, a study by T. Ozturk et al. proposes a DL model to detect COVID-19 patients by analyzing Chest X-ray images. This created system relies on DarkNet technology for accurate forecasting of convolutional layers. The goal of this research is to determine radiology as a means of verifying the scan procedure. Radiologists have assessed the heat maps generated by automated models. To test the functionality of the created method, developers have used five-fold cross-validation. The highest level of accuracy has been achieved and reported for both binary and multi-class classifications (Ozturk et al., 2020).

S. Vaid, et al. carried out another study in Vaid et al. (2020) to improve the accuracy of the reported COVID-19-positive cases and to predict the virus using Chest X-ray images using DL models. This system employs a Convolutional Neural Network (CNN) to detect structural defects and illness classification that was crucial in revealing hidden patterns. This system used public datasets available on the internet. Similarly, in Apostolopoulos and Tzani (2020), I. Apostolopoulos and T. Mpesiana also proposed a transfer learning model that leverages the power of pre-trained VGG19 and MobileNet v2 models to analyze Chest X-ray images. The objective was to predict and identify patients with pneumonia and COVID-19 automatically. The authors used two datasets, containing chest X-ray images of patients infected with normal pneumonia and COVID-19, obtained from open sources. The study employed tenfold cross-validation to assess the performance of the presented techniques. Both VGG19 and MobileNet v2 exhibited higher accuracy rates for binary classification. Whilst the first dataset demonstrated the highest accuracy for the multi-class classification, the MobileNet v2 was employed in the second dataset to obtain optimum accuracy in binary and multi-class classification.

According to Panwar et al. (2020), it has been concluded that a robust COVID-19 screening model requires DL-NN. The proposed framework uses CXR images and is based on nCOV-net. The dataset includes CXR images of COVID-19-positive and healthy patients. To assess the efficacy of the proposed approach, random sampling is applied

to both the training and testing datasets. Finally, the unique projected technique for binary classification shows a high level of accuracy.

Consequently, the early and effective identification of COVID-19 patients has become one of the crucial requirements. As emphasized in the UN sustainability goals, leveraging ICT technologies can significantly enhance “good health and well-being”. Addressing this problem, the scientific contribution of this study can be outlined as follows: (1.) Introducing a contactless method for analyzing cough sounds to discern their resemblance to a COVID-19-positive cough. (2.) Implementing a contactless approach to analyze a person’s respiratory rate and identify signs of shortness of breath using DL and IoT-based technologies for the detection of COVID-19 patients. (3.) Identifying and utilizing the most suitable DL model tailored to the specific context of Sri Lanka. Those interested in further advancing this study can contribute by visiting the GitHub repository available [here](#).

2. Background study

Artificial Intelligence (AI) with emulated hardware systems is widely used nowadays for different purposes. Almost all industries are increasingly moving towards AI combined with emulated hardware solutions as technology develops to address their problems (Jiang et al., 2022; Punla and C. Farro, 2022; Yamasinghe et al., 2022; Chandio et al., 2022). As a result of the Coronavirus’s spread, several studies are currently being conducted around the world to address this issue using AI.

2.1. Use of deep learning models for cough classification

Cough is a common symptom of most respiratory system-related diseases (NA, 2020). Furthermore, AI models have been developed to detect different respiratory diseases such as pneumonia and Tuberculosis (Monge-Álvarez et al., 2019; Botha et al., 2018).

Similarly, when considering COVID-19, cough is one of the most common symptoms with more than 59% of the symptomatic patients experiencing it. It is common for COVID-19 to impact the respiratory system, which can change how someone breathes, coughs, and speaks. According to the ZOE COVID Symptom Study app, persistent cough can be an early symptom of COVID-19. A patient may be diagnosed with the virus even if they do not have a chronic cough.

People diagnosed with the Coronavirus can also be asymptomatic. However, the Massachusetts Institute of Technology (MIT) claims that even asymptomatic patients can be diagnosed by analyzing cough sounds. Several research studies have been undertaken and are still being conducted to analyze cough sounds to identify COVID-19 patients.

An AI framework created by J. Laguarda, F. Hueto, and B. Subirana extracts biomarker characteristics from cough recordings to pre-screen for COVID-19. In this system, the Mel Frequency Cepstral Coefficient is used to modify cough recordings before they are input into a Convolutional Neural Net(CNN)-based architecture with a Poisson biomarker layer and three pre-trained ResNet50’s working in parallel to produce a binary pre-screening diagnostic. Despite starting from scratch with a machine learning model to identify Covid-19 patients by cough, they fell short of their goals due to a lack of accuracy. As a result, they put it to the test using an existing AI model that was meant to assess Alzheimer’s disease and found it to be more accurate. This system performs the analysis using a mobile application and only considers the cough when arriving at the final decision (Laguarda et al., 2020).

A similar study conducted by A. Imran et al. introduced a mobile application to pre-screen for COVID-19 using cough sounds. The system classifies the cough into three categories: negative, positive, and inconclusive. It derives this classification by comparing the pathological changes in the respiratory system caused by COVID-19 infection to those caused by other respiratory illnesses. As with the previously mentioned study, it considers the cough as the sole factor when determining the conclusion (Imran et al., 2020). The study “Virufy”,

Table 1
Summary of available systems that detect potential COVID-19 patients by analyzing cough sounds.

Author/s	Dataset	Accuracy	Consider other symptoms (except cough)
Laguarta et al. (2020)	Crowdsourced COVID-19 dataset	Symptomatic - 94.2% Asymptomatic - 83.2%	X
Imran et al. (2020)	Data collected using a mobile application	92%	X
Chaudhari et al. (2020)	Crowdsourced COVID-19 dataset	77.1% (ROC-AUC)	X
Pal and Sankarasubbu (2020)	Crowdsourced COVID-19 dataset	95.04%	X
Ismail et al. (2020)	Crowdsourced COVID-19 dataset	91.2% (ROC-AUC)	X
Quatieri et al. (2020)	Crowdsourced COVID-19 dataset	-	X

Table 2
Summary of available systems that detect shortness of breath (O - included, X - Not included).

Author/s	Privacy	User experience	No environmental impact	Contactless	Reusability	Safety
Massaroni et al. (2019)	X	X	O	O	O	O
Wang et al. (2019)	O	O	X	O	O	X
Krug et al. (2016)	O	X	X	O	O	O
Luis et al. (2014)	O	X	O	X	O	O
Panahi et al. (2020)	O	O	X	X	O	O
Liu et al. (2021)	O	O	O	X	O	O
Understanding (2022)	O	O	O	X	X	O
Mukhtar et al. (2021)	O	O	O	O	O	X
Laguarta et al. (2020)	O	O	O	O	O	X

carried out by G. Chaudhari et al. shows that an AI-based method can identify possible COVID-19 patients via crowd-sourced cough audio clips. This system has obtained a ROC-AUC of 77.1%. Just as the prior study, it employs a mobile application to record the cough sound and considers the cough as the sole factor when concluding (Chaudhari et al., 2020).

Another approach, developed by A. Pal and M. Sankarasubbu, uses an AI framework to analyze cough sounds to identify COVID-19 patients. The coughing sound is further divided into four categories: healthy, asthma, bronchitis, and COVID-19. For both COVID-19 negative and positive cough identification, this approach has achieved accuracies of greater than 89%. However, this system has only considered 328 coughs from 150 patients to carry out the study (Pal and Sankarasubbu, 2020). M. Al Ismail, S. Deshmukh, and R. Singh proposed to test the theory and quantitatively describe the observed alterations to detect COVID-19 from voice. A dynamical system model for the oscillation of the vocal folds is used for this purpose, and a newly developed ADLES algorithm is used to produce vocal fold oscillation patterns directly from recorded speech. This is another system that only considers coughs to detect whether a person is infected with the Coronavirus (Ismail et al., 2020).

T. Quatieri, T. Talkar, and J. Palmer have also presented a framework for identifying COVID-19 vocal biomarkers through speech production techniques such as breathing, vocalizations, and pronunciation (Quatieri et al., 2020). In the study, Mukhtar et al. (2021) an SW-420 sensor was utilized to detect cough and its variations throughout the study. To detect cough, the system employs Doppler radar, continuous-wave (CW) radar, and vibration detection, with the hardware or sensor mounted to the front of the person's neck, which makes the person uncomfortable.

Unfortunately, most published research is limited to non-open-source datasets, hence it is difficult to assess the capacity of these algorithms to detect COVID-19 using arbitrary cough recordings. Table 1 depicts a summarized description of the papers. Models trained on clinical data have a significant chance of failing to generalize, specifically when testing data using crowd-sourced data and collecting audio samples in a variety of settings, often with background noise.

2.2. Background of detecting shortness of breath

The utilization of contact-based methods for monitoring respiration rate has been associated with a slew of issues. Consequently, researchers have redirected their efforts towards developing a novel contactless approach, which involves capturing video footage of the patient's chest, to monitor the human respiratory rate. Based on the published research to date, it is evident that for contactless energy to operate accurately, either the movement of the chest or the person's breath must be considered.

As given in Table 2, subsequently, multiple systems have been introduced, each with its limitations as documented in the literature. Carlo Massaroni et al. in Massaroni et al. (2019) used an RGB camera to record video of the subject's chest movement, adhering to the approach in research. Additionally, the system utilized the color intensity produced by the individual as input. However, the reading may vary based on the subject's clothing, as garments with multiple colors may not consistently reflect the same intensity of color. Furthermore, the system is built on the assumption that slim-fit clothing allows for the complete transfer of chest wall movement to the side, whereas loose-fit clothing only permits partial transfer. Further, as most people are uncomfortable with video filming their chest, this could result in a privacy concern.

Wang et al. (2019) used cutting-edge physics in their research. The system utilized the Doppler effect and air turbulence. According to the authors, the system emitted a sound wave to identify the Doppler effect caused by exhaling airflow. As a result, to eliminate external airflow and noise, the system requires tightly-confined space. Even though it can be kept in a closed environment, it cannot be integrated with a system with other hardware components due to the noise that may be produced. As a result, there is a chance that the outcome will be inaccurate. In the case of the study conducted by Johannes W. Krug et al. in Krug et al. (2016), a laser must be pointed at the person's chest. Because people's heights vary, it may be necessary to adjust. In addition, the authors state that "the test individual must wear skin-tight clothing". As a result, it also caused the same problem incurred in Massaroni et al. (2019) and failed to provide a pleasant user experience.

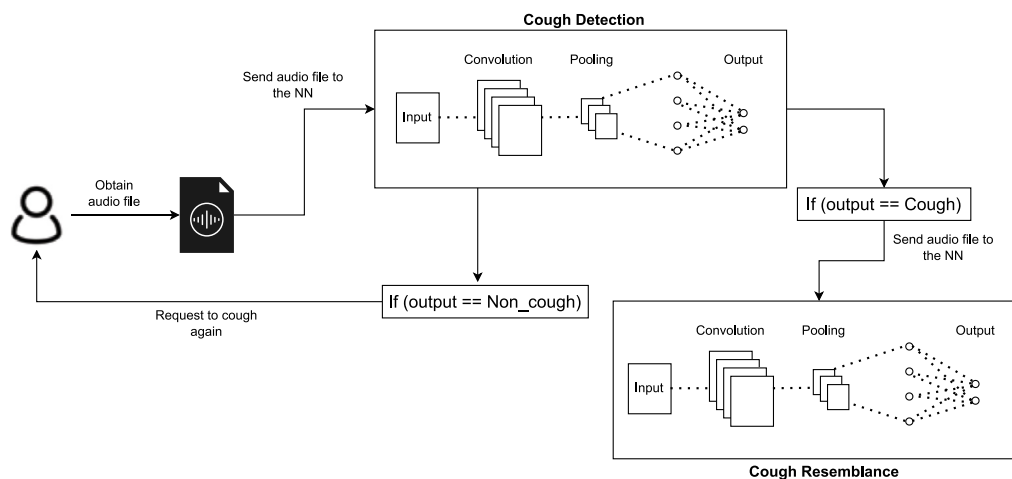


Fig. 1. Component overview — COVID-19 cough classification.

Even though developing a smart sensor is effective, it still needs to be in contact with the person, according to research by Luis et al. (2014). As mentioned by the authors, the device is also designed to be used while the participant is lying in bed since it is not possible to use the system in other environments. The same challenge related to contact-based approaches was presented in the study conducted by A. Panahi et al. as shown in Panahi et al. (2020). Furthermore, as the authors pointed out, humidity might impact the system. Consequently, there can be misleading readings because the test subject may be sweaty. Aside from these drawbacks, contact-based technology is not appropriate during a pandemic.

In the study by Liu et al. (2021), the apparatus is mounted on a bed to obtain readings of respiratory rates. As a result, this technique was reliant on a second surface that is in direct contact with the test subject. Unfortunately, the sensor does not come into direct contact with the person, and it is unable to be employed in a pandemic situation due to its reliance on the other surface. A novel solution for integrating a thermistor into the facemask was presented in the study by R. Bhattacharaya et al. in Bhattacharya et al. (2017). This approach is more suitable for individual use. However, it is unrealistic to anticipate that this mask will be affordable to all the company's employees. Given the need to change the face masks regularly (at least once a week), the thermistor cannot operate for an extended period. Aside from that, this method does not have a monitoring capability where the organization can monitor the employee's respiration rate.

Even though the study proposed by Alkali et al. (2014) maintains a contactless approach, the hardware component must be placed sufficiently close to the person's nasal area. Therefore, the end that is exposed to the person may contain virus particles transmitted through an infected person. Hence, it is not safe to use during a global pandemic.

In the study by Min et al. (2010), an ultrasonic module is combined with many other sensors to provide a contactless technique to monitor the respiratory rate. Ultrasonic sound, on the other hand, can potentially harm the human ear. As a result, it cannot be considered a safe system to use regularly. Further, the system should maintain a minimum distance of 100 cm, as stated by the authors. As a result, the system may take up more space.

Yet with regard to the technical difficulties and privacy concerns, this study discusses a contactless method utilizing two cameras, i.e., thermal and web, mounted together for detecting shortness of breath in 30 s. Further discussion can be found in Section 3.2.

3. Materials and methods

This chapter explains the materials and procedures used in this study in two sections: cough classification and shortness of breath detection.

3.1. Cough classification

The process of cough classification comprises two stages: Cough Detection and Cough Resemblance. Initially, the audio of a person's cough is captured for a duration of 5 s using the 'sound-device' Python library, for a single channel. Next, the audio is converted into a Mel-spectrogram (Understanding, 2022), which serves as the basis for determining the presence of a cough (referred to as cough detection). If a cough is identified in the audio, the spectrogram is further analyzed to assess its resemblance to COVID-19-positive coughs (referred to as cough resemblance). This procedure is illustrated in Fig. 1. More details of the two stages are discussed in the subsequent sub-sections.

Cough detection is carried out via transfer learning on a CNN. To choose the best outcome, three pre-trained models: VGG-16, EfficientNet, ResNet, and Inception-V3, were used and tested in this study. All these models are configured with similar parameters. Overall, all these models are trained with a training dataset of 2704 and a validation set of 676 spectrograms as explained in Section 3.1.1.

The more important step in Cough Classification is cough resemblance, which aims to determine whether the captured cough is positive or negative for COVID-19. This step specifically focuses on the spectrograms that were identified as containing a cough during the cough detection phase. Similar to cough detection, cough resemblance utilizes transfer learning, employing the same pre-trained models for analysis.

3.1.1. Data collection

The cough classification process involves the utilization of two Convolutional Neural Networks (CNNs): one for cough detection and the other for cough resemblance.

Consequently, two distinct datasets were employed for this purpose. The first dataset, referred to as the cough detection dataset, was obtained from open-source datasets such as Coswara (Github, 2022a) from the Indian Institute of Science, Coughvid (Orlandic et al., 2022) from EPFL Switzerland, and the ESC-50 dataset (Github, 2022b). The second dataset, known as the cough resemblance dataset, was created by combining data from Coswara, Coughvid, and Kaggle datasets. Detailed descriptions of the datasets are included in Table 3. For cough detection, the ESC-50 dataset that contains 50 classes of environmental audio recordings was utilized. This dataset provided audio samples labeled as "coughing", which were used for training the neural network to identify the presence of coughs in the audio. A total of 3380 audio files were utilized in the cough detection phase, with the training and validation sets split in an 80:20 ratio. This resulted in 2704 training audio files and 676 validation audio file samples.

In the context of cough resemblance, the Coswara dataset (as shown in Table 4) contained 343 samples with the COVID-19 positive audio files labeled as 'positive mild', 'positive moderate', and 'positive

Table 3
Dataset classification (Training and Testing set) for both components in this system.

	Total	Training set	Testing set
Cough detection	3380	2704	676
Cough resemblance	3000	2400	600

Table 4
Detailed classification of the data used for cough resemblance.

Dataset	Status		Number
Coswara	COVID-19 Negative	Healthy	710
		No_resp_illness_exposed	120
		Resp_illness_not_identified	80
		Recovered_full	40
		COVID-19 Positive	positive_mild
	Positive_moderate	123	
	Positive_asymp	118	
Coughvid	COVID-19 Negative	Healthy	550
	COVID-19 Positive	COVID-19	808
Kaggle	COVID-19 Positive	Positive	349
Total - Positive			1500
Total - Negative			1500
Total			3000

asymptomatic'. Additionally, 950 files with different statuses were categorized as COVID-19 negative audio files. Each entry in this dataset consisted of two cough audio files: shallow cough and heavy cough. However, for this study, only the heavy cough audio files were utilized.

To ensure a balanced training dataset, 808 audio recordings with the label 'COVID-19 Positive' were assigned to the positive class, while 550 other audio files from the 'Coughvid' dataset were assigned to the negative class. Furthermore, an additional 349 positive coughs were obtained from Kaggle (Larxel, 2021). Overall, this study utilized a total of 3000 audio files for cough resemblance and 3380 for cough detection, with an 80:20 ratio for training and validation. The distribution of the data used for cough resemblance is also visualized in Fig. 2.

In addition to the data collected from the aforementioned sources, a specific focus of this study was to assess the cough resemblance within the Sri Lankan population. To achieve this, a set of 54 audio files containing cough sounds was obtained from members of the Sri Lankan community. The dataset (Liyanarachchi et al., 2023) can be accessed for further reference and examination (dataset). Classification of these cough audios is shown in Fig. 3. The audio files collected for these datasets were pre-processed to obtain Mel-spectrograms as spectrograms are being analyzed in this study. All these spectrograms were then resized to 224 × 224 pixels since this study uses CNN to achieve its outcomes.

The authors noted a few limitations when considering the available datasets. A main limitation was the small number of COVID-19-positive cough samples. However, given the current state of affairs regarding the propagation rate of the diseases, it is also recon that there was no safe way to get the data from the doctors or a third party on our own. Thus the larger part of the data had to be obtained through crowd-sourced online datasets.

3.1.2. Pre-processing data

As mentioned previously, the datasets used in this component contain labeled audio files. As the initial step, the dataset used for the CNN to get a cough resemblance was divided into 'healthy' and 'positive'. Similarly, the other dataset used for cough detection was divided into the 'cough' and 'non-cough' categories. Subsequently, Mel-spectrograms were generated from the audio files of both datasets. To accomplish this, the Librosa and Matplotlib Python libraries were utilized. All spectrograms were converted to RGB format and resized to 224 × 224 dimensions. However, when these datasets were input into the CNNs, the Mel-spectrograms were converted to a NumPy array containing the features and the label.

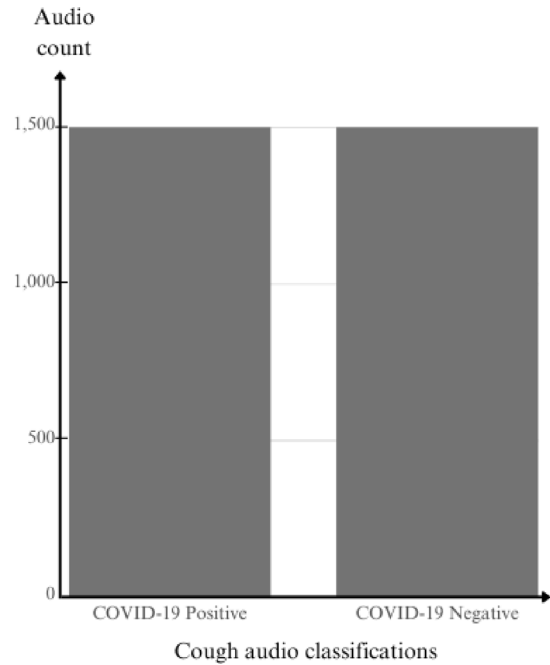


Fig. 2. Training dataset classification of cough resemblance.

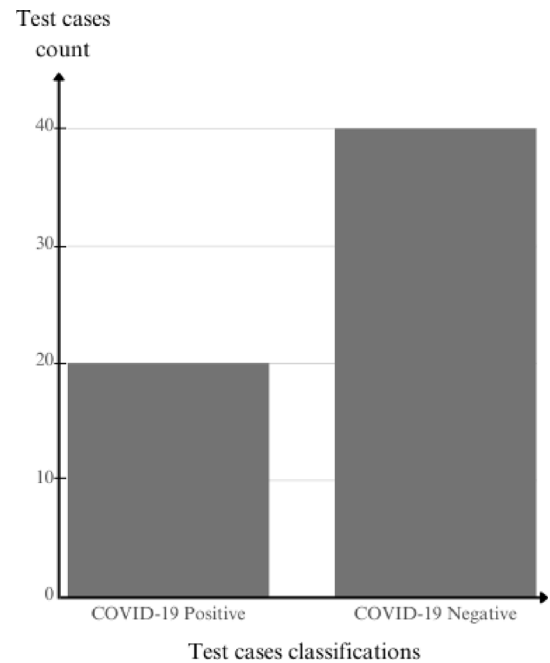


Fig. 3. Testing set classification of Sri Lankan data.

3.1.3. Metrics

The metrics discussed in Table 5 are recorded in relation to the CNNs' categorization tasks for both cough detection and cough resemblance computation models. The performance of these models is evaluated using the following metrics for classifications.

- Precision - Positive predictive value - Precision is the degree to which your model is precise/accurate in terms of how many of the predicted positives are actually positive.

$$Precision = TP / TP + FP \tag{1}$$

Table 5
Specific Metrics for classification tasks of CNNs.

	Cough detection	Cough resemblance
True Positive - TP	Cough identified correctly	Correctly identified COVID-19 positive patient
False Negative - FN	Cough identified incorrectly	Incorrectly identified COVID-19 positive patient
True Negative - TN	Non-cough identified correctly	Correctly identified COVID-19 negative patient
False Positive - FP	Non-cough identified incorrectly	Incorrectly identified COVID-19 negative patient

- Recall – True positive rate

$$Recall = TP / (TP + FN) \quad (2)$$

- F1 score - Used to find the balance between Recall & Precision

$$F1score = 2 * (Precision * Recall) / (Precision + Recall) \quad (3)$$

where, TP — True Positive, FP — False Positive, and FN — False Negative.

3.1.4. Transfer learning

Transfer learning is the process of using a previously learned model to solve a new problem. Large datasets are frequently used to train pre-trained models. The weights calculated by these models can be used on new models which lack large datasets. It is possible to utilize these models directly to make predictions on new tasks or to incorporate them into the process of training for a new model. Incorporating pre-trained models into a new model reduces training time and generalization error. There are six common steps to follow when implementing transfer learning:

1. Get a pre-trained model
2. Create the base model
3. Freeze layers
4. Add new trainable layers
5. Training the new layers on the dataset
6. Improve the model using fine-tuning.

Four separate pre-trained models were considered for this system via the ‘Keras’ Python library. The CNNs considered for this system were VGG16, Inception v3, ResNet, and Efficient-Net. These CNNs were used for both cough detection and cough resemblance models. Some hyperparameters were shared across all CNNs. All the convolutional layers of these models were activated by the Rectified Linear Unit (ReLU). To mitigate overfitting, a Dropout layer was added to the neural network with two hidden layers. The Adam optimizer, known for its efficiency and flexibility, was utilized with a learning rate of 0.0001. All the layers of the CNNs were configured to be non-trainable, and the two models were completed with a Binary cross-entropy loss function. The shared hyperparameters in the context of neural networks include the Rectified Linear Unit (ReLU) activation function, which introduces non-linearity by mapping negative values to zero and preserving positive values. Dropout, another technique, aids in regularization by randomly setting a fraction of input units to zero during training, promoting more robust and generalized representations. The Adam optimizer combines the strengths of AdaGrad and RMSProp by adaptively adjusting the learning rate for each parameter. Additionally, a learning rate of 0.0001 was selected for improved efficiency and flexibility in determining the step size during optimization iterations. These hyperparameters collectively contribute to the efficacy of training and regularization of neural networks.

The following is a brief overview of the pre-trained models employed and how they were applied in this study:

- VGG16 is a Convolutional Neural Network model that has achieved an accuracy of 92.7% of top-5 test accuracy in ImageNet (a dataset containing 14 million images in 1000 classes) (Simonyan and Zisserman, 2014). This model uses input RGB images of a fixed size of 224×224 . In this study, this model was initially

fine-tuned with Keras and is used in both components, Cough detection and Cough resemblance computation. The output layers were made non-trainable by freezing the weights, and other trainable parameters in each layer were similarly made not to be trained or altered when my dataset was fed.

- Inception-v3 is a convolutional neural network design from the Inception family that includes Label Smoothing, Factorized 7×7 convolutions, and the inclusion of an auxiliary classifier to transport label information deeper down the network, among other improvements (Szegedy et al., 2016). For the process of identifying the best pre-trained model for the two models in this study, the Inception v3 pre-trained model was also used. To avoid over-fitting and to make sure that the model does not memorize the exact details of the training images, we also employed data augmentation for the training dataset.
- EfficientNet was the other pre-trained model that was used in this study for the purpose of training the two models. This is a convolutional neural network design and scaling method that uses a compound coefficient to consistently scale all depth, width, and resolution dimensions (Panwar et al., 2020). A new output layer with two nodes corresponding to ‘cough’ and ‘non-cough’ in the cough detection model and ‘positive’ and ‘healthy’ in the cough resemblance model was added to this model.
- ResNet (He et al., 2016) is a pre-trained model commonly used in deep learning for computer vision tasks. It uses residual blocks to enable the training of much deeper networks, which in turn helps to improve the accuracy of the model. In this study, ResNet was used as one of the pre-trained models for training two separate models, one for cough detection and the other for cough resemblance. The ResNet model was fine-tuned for the task by adding a new output layer with two nodes, one for ‘cough’ and the other for ‘non-cough’ in the cough detection model, and one for ‘positive’ and the other for ‘healthy’ in the cough resemblance model. The pre-trained ResNet model was modified and retrained using a transfer learning approach to make accurate predictions for the specific tasks at hand.

3.1.5. Testing

Both functional and non-functional testing was carried out as follows:

- **Functional Testing:** The functional testing process for the cough detection system involved different stages. Initially, unit testing was performed to ensure the proper functioning of individual components such as cough recording, spectrogram generation, cough detection, and cough resemblance. These components were tested separately and were found to be working as expected. Next, integration testing was conducted to combine and test the cough detection and cough resemblance components in combination, ensuring their seamless functionality in conjunction. Regression testing was conducted after each code modification to ensure the stability and functionality of existing features. This type of testing is essential to maintain system stability during continuous improvement. System testing, the final stage, involved joining the completed components together and testing the complete system as one unit to verify the attainment of desired results. Overall, the testing process encompassed unit testing, integration testing, regression testing, and system testing to ensure the accuracy and effectiveness of the cough detection system.

Table 6
Average execution time and peak memory consumption.

Function	Functionality	Average peak size (MB)	Average time elapsed (ms)
Spectrogram creation	Create the spectrogram using the previously recorded audio file.	167.95	2499.56
Cough resemblance	Load the two models used in the system. Check if a cough is present in the audio. Provide the final result of whether or not the cough is COVID-19 positive.	141.79	1136.81

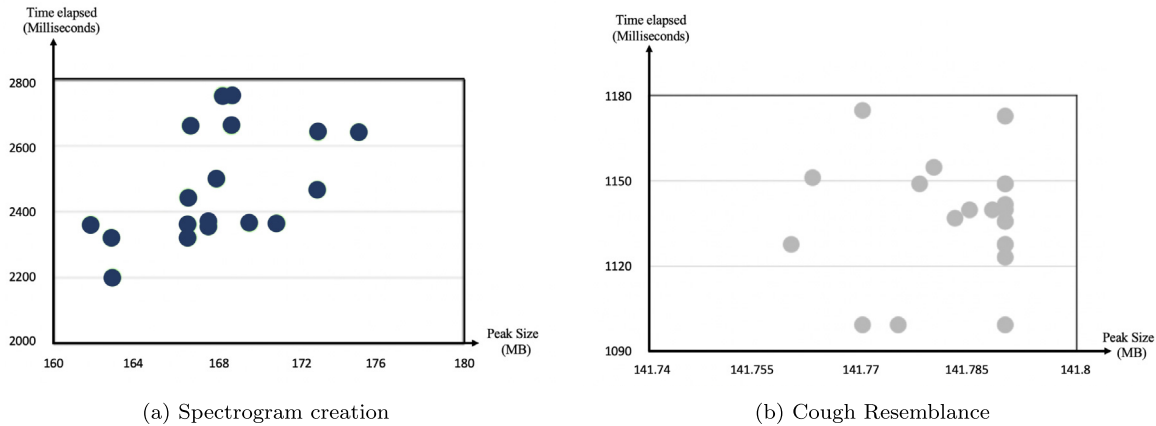


Fig. 4. Scatter plot for functional performance.

- **Non-Functional Testing:** The reliability of the system was tested to ensure consistent output, specifically in determining if the recorded cough is COVID-19 positive or not, while performance testing involved evaluating execution time and memory consumption for functions related to spectrogram creation and cough resemblance, with results summarized in Table 6 and represented visually in Figs. 4(a) and 4(b).

3.2. Shortness of breath detection

Shortness of Breath is the second component of this study of detecting COVID-19-positive patients. It is found that shortness of breath is a vital symptom of COVID-19. Hence detecting this symptom was considered in this study. An overview of this component is depicted in Fig. 5.

The steps outlined below are used to detect shortness of breath in this study.

- Identifying the nostril area
- Detecting the inhalation and exhalation
- Counting the number of thermal color changes.
- Comparing the obtained count with the respiration rate of a healthy person

3.2.1. Hardware component

As for the hardware components in this part of the study, a camera setup was used. A thermal camera and a standard web camera are mounted on top of each other and the focus of these two cameras should be almost identical in every way. In this study, a web camera with a resolution of 1280×720 pixels and a FLIR C2 camera was used. The setup of the two cameras is depicted in Fig. 6

3.2.2. Capturing breathing pattern

Initially, the two cameras capture the person's face using the Python libraries; 'Dlib' and OpenCV. This 'Dlib' library includes a pre-trained machine learning model that includes 68 facial landmarks. The model "shape predictor 68 face landmarks.dat" was loaded into the system

at the very beginning. This file was then used to create an instance of Dlib's shape predictor class, which contains all of the functionality for identifying and extracting facial features. The x and y coordinates of the facial landmarks were then determined using the processed frame and the previously recognized face. The received file was then converted to a Numpy array, which contains the x and y coordinates of facial landmarks. These coordinates are given in Fig. 7.

Even though the facial landmark identification and processing were done using a standard web camera, these frames, however, do not carry any information concerning the person's respiration. Therefore, a thermal camera was employed to gather such specifics. However, due to the lack of rich features in the thermal camera footage, extracting features (Nostril region) was infeasible. Though there are numerous alternative methods available for extracting information from a thermal image, the consistency was uncertain due to the person's movements.

Consequently, to provide a better alternative, the proposed system used both cameras to extract key characteristics from the thermal image. The steps are as follows,

- The web camera was utilized to recognize and locate the x and y coordinates
- The x and y coordinates of the nostril area were extracted.
- Then the extracted x and y coordinates of the nostril area are added to the frame obtained from the thermal camera

However, even if the relevant starting and ending points for the nostril area are 32 and 36, respectively (Refer Fig. 7), achieving a proper view is unlikely. As a workaround, the facial landmark number 30 is used as the beginning point.

3.2.3. Detecting the inhalation and exhalation

When the footage from the FLIR C2 thermal camera was examined, it was observed that during a person's breathing, it exhibits a temperature difference in green at the nasal area as depicted in Fig. 8. According to the calibration of the FLIR thermal camera, the green hue represents relatively low temperatures. On the other hand, there is no thermal color difference in the nose area during exhalation because the temperature of the exhaled air is the same as the person's body temperature. As a summary, the appearance of green color pixels is interpreted

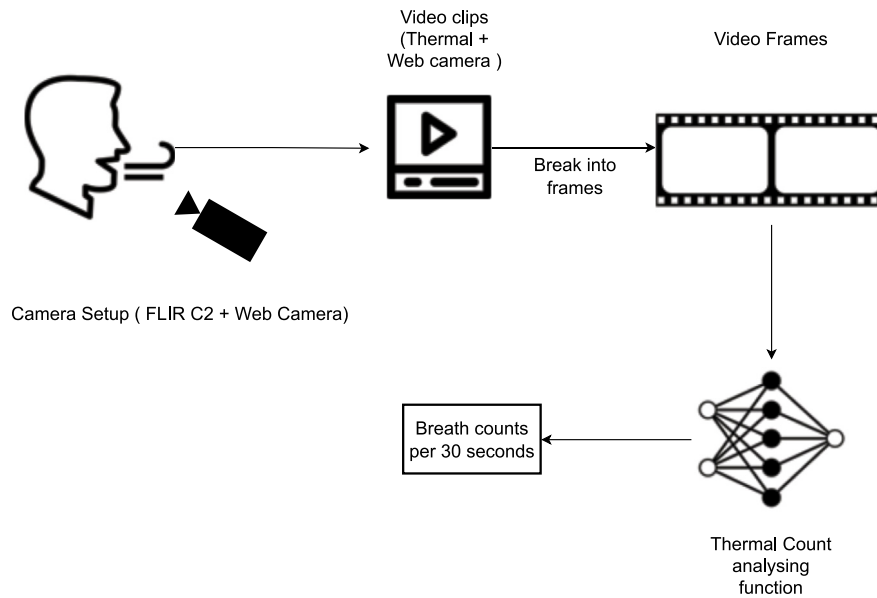


Fig. 5. Component overview — Shortness of breath detection.



Fig. 6. Shortness of breath detection — Hardware setup.

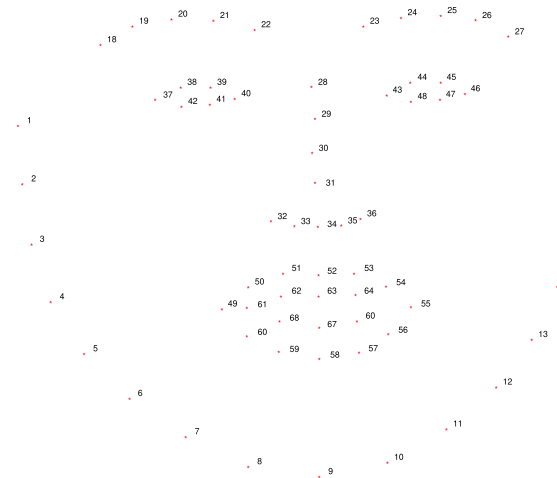


Fig. 7. Facial landmarks from 'Dlib' Library.

as a human inhale and the disappearance of the same-colored pixels as an exhale. Consequently, the total number of complete breathing cycles was calculated by counting the number of color changes on the extracted region of the FLIR C2 thermal camera.

3.2.4. Counting the number of thermal color changes

The RGB color-modeled image was first converted into an HSV (Hue, Saturation, Value) color-modeled image. The HSV color scale produces a numerical representation of the image that corresponds to the color names. Using these numerical values, a program can easily identify and extract areas for a given color. However, after several test runs, it was discovered that the thermal color change can vary from green to yellowish green depending on the temperature of the environment. Hence, the standard HUE values were inadequate to detect color changes. To develop a solution, various experiments were carried out under typical room temperature in the coastal area of Sri Lanka by varying the boundary hue values. This area was selected, because the number of patients in the coastal area was high and the spreading ratio was also high. Finally, the upper boundary hue value was determined to be 110, while the lower boundary hue value was found to be 30 for this study. A binary image was then generated by providing the aforementioned two boundary values, along with the HSV color-modeled images. As illustrated in Fig. 9, the pixels within



Fig. 8. Thermal color difference during inhalation.

the boundary were then converted to white (pixel value change to 255), while the rest of the pixels were converted to black (pixel value change to 0).

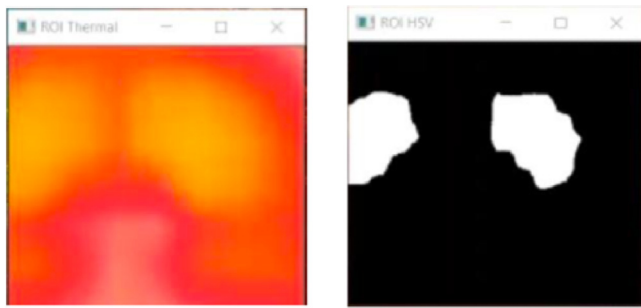


Fig. 9. Thermal and binary views of the Nostril during an inhalation.

Algorithm 1 Algorithm to count the thermal color differences

```

previous_frame ← 0
breath_count ← 0
while time.now < time.now + 30seconds do
    max_pix ← maximum_pixel_of_binary_image
    if max_pix == 255 then
        previous_frame ← 255
    else
        if previous_frame == 255 then
            breath_count ← breath_count + 1
        end if
        previous_frame ← 0
    end if
end while

```

Finally, Algorithm 1 was used to count the respiratory cycles. As it must first determine the maximum pixel value existing in the binary image, the binary image which has pixel values of 0 or 255, 255 would assign to max_pix , if a white region is present. Otherwise, the value will be set to 0. Then, if the max_pix value equals 255, then the value 255 is assigned to the $previous_frame$ variable. It is necessary to retain information from the previous frame in order to recognize the transition from inhalation to exhale. Because a single inhalation process contains multiple frames. The loop was then resumed, and the program would keep the $previous_frame$ variable value unchanged until there is a white region in the image.

At the very first movement of the exhalation, the value of the max_pix variable was replaced by 0 as there was no white region present in the frame. Yet, the value of the $previous_frame$ variable is still set to 255. In this situation, the if condition of the 5th line becomes false and the *else* part in line 7 is executed. Within the *else* condition in line 7, it checks the value of the $previous_frame$ variable. Since the current frame does not contain a white region (max_pix set to 0) and the previous frame has had a white region ($previous_frame$ set to 255), it indicates a transformation of color. In this way, the system identifies the transformation from inhalation to exhalation. Since the program is focused on counting the total number of inhalations, this transformation needs to be counted. Therefore, within the nested, if condition, the value of the $breath_count$ variable is increased by one. Then immediately the value of the $previous_frame$ is set to 0 denoting continuations of the exhalation process. Note that all these computations were carried out based on the first frame as the exhalation. However, for the inhalation process, there are multiple frames regarding a single exhalation and the value of the max_pix is set to 0. Therefore, the outermost and the nested *if* conditions will fail throughout the exhalation. As a result, the value of the $breath_count$ variable would not be updated until the person's exhalation is complete. The values were changed as the individual begins to inhale again and the value of the $breath_count$ will be incremented by one at the very first movement of the exhale. This process continues until the loop stop after 30 s, and at the end of

Table 7
Accuracy comparison for cough detection.

Model	Average Accuracy(%)
VGG-16	98.0
ResNet	97.4
Inception V3	93.6
EfficientNet	87.0

Table 8
Accuracy comparison for cough resemblance.

Model	Average Accuracy (%)
ResNet	93.17
VGG-16	92.4
EfficientNet	86.4
Inception V3	82.7

Table 9
Summary of tested scenarios for cough resemblance.

Test case	Symptomatic/Asymptomatic	Nationality	Result	Confidence
COVID Patient	Symptomatic	Sri Lankan	Positive	90.73%
COVID Patient	Asymptomatic	Sri Lankan	Positive	91.30%
COVID Patient	Symptomatic	Indian	Positive	85.10%
COVID Patient	Asymptomatic	Indian	Positive	91.31%
A healthy person	-	Sri Lankan	Healthy	98.27%
A healthy person	-	American	Healthy	99.14%

the loop, the $breath_count$ variable can be used to get the number of complete breathing cycles of the person for 30 s.

3.2.5. Comparing with the respiration rate of a healthy person

The obtained reading of the respiration rate must then be compared to the average respiration rate of a healthy person in the final stage. According to Hopkins Medicine, a healthy adult's average rate of breathing is between 12 and 16 breaths per minute.

4. Simulation implementation and testing

The training and testing for all models in this study were conducted on a MacOS device with a 6-Core Intel Core i7 processor and a memory of 16 GB.

4.1. Cough classification

As mentioned in Section 2, three pre-trained models were experimented with to get the highest validation accuracy for both cough detection and resemblance. Tables 7 and 8 show the comparison of the four models for Cough detection and Cough resemblance respectively. Moreover, the training and validation accuracy plots for cough resemblance are depicted in Fig. 11. The outputs show that although the accuracies of these trained models are high, some of them have overfitted data. This resulted in the models not being able to generalize well to new data. Therefore, after analyzing the comparison of these models, the model with the highest accuracy, i.e., the VGG-16 model for cough detection and ResNet for cough resemblance was selected. As depicted in Tables 7 and 8, the models achieved accuracies of 98% and 94% respectively for the two sub-components (see Fig. 10).

Tables 10 and 9 shows several test cases that represent the full dataset for the two components, detection, and resemblance respectively that were carried out with the models that were fine-tuned and developed using the ResNet model.

4.2. Shortness of breath detection

After following the steps discussed in Section 2 the implementation was tested using 20 people. The sample set is explained in Fig. 12.

	precision	recall	f1-score	support
healthy	0.91	0.89	0.90	300
positive	0.95	0.95	0.94	300
accuracy			0.93	600
macro avg	0.93	0.92	0.92	600
weighted avg	0.93	0.93	0.93	600

Fig. 10. Classification report — Cough resemblance (ResNet).

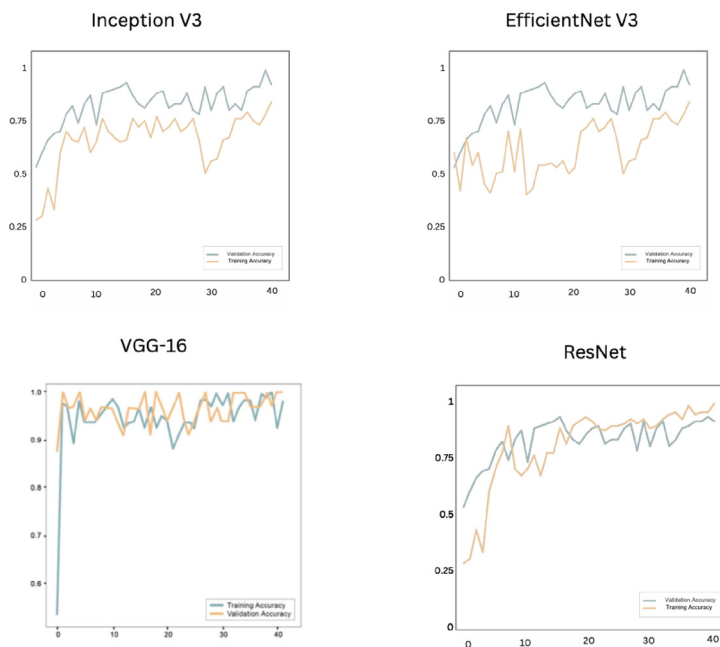


Fig. 11. Training and validation accuracy plots of the three CNNs for Cough Resemblance; X-axis: Number of Epochs, Y-axis: Accuracy.

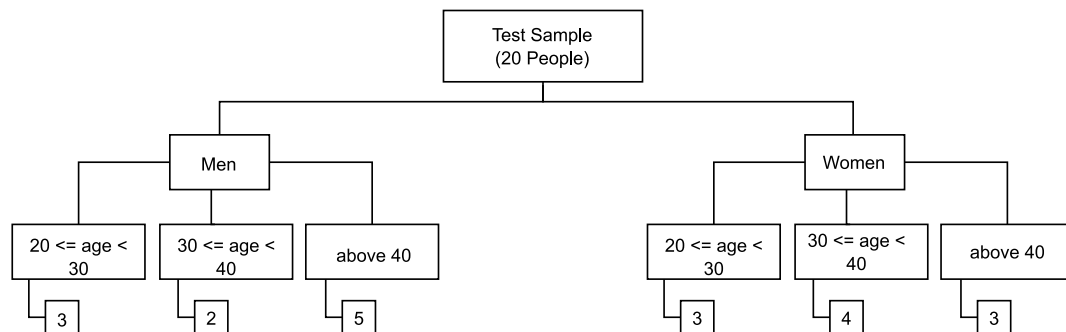


Fig. 12. Testing sample for shortness of breath.

This component was tested independently for all the steps described in Section 2.2 of this paper. The nostril identification was 95% accurate, Furthermore, 100% accuracy was attained for inhalation and exhalation detection. Finally, it was obtained a 90% accuracy for thermal change count with 18 successful test cases. All of these observations are based on the above-mentioned test sample and were carried out at an average room temperature in Sri Lanka’s coastal region.

5. Results & discussion

5.1. Results

5.1.1. Cough classification

Cough detection classifies a given audio as ‘cough’ or ‘non-cough’ while cough resemblance classifies it as ‘positive’ or ‘healthy’. The three

Table 10
Summary of tested scenarios for cough detection.

Test Case	Expected	Actual	Confidence
A female cough	Cough	Cough	98.02%
A male cough	Cough	Cough	99.73%
No sound at all	Non-cough	Non-cough	99.22%
A female talking	Non-cough	Non-cough	94.89%
A male talking	Non-cough	Non-cough	95.03%
Dog barking	Non-cough	Non-cough	92.96%

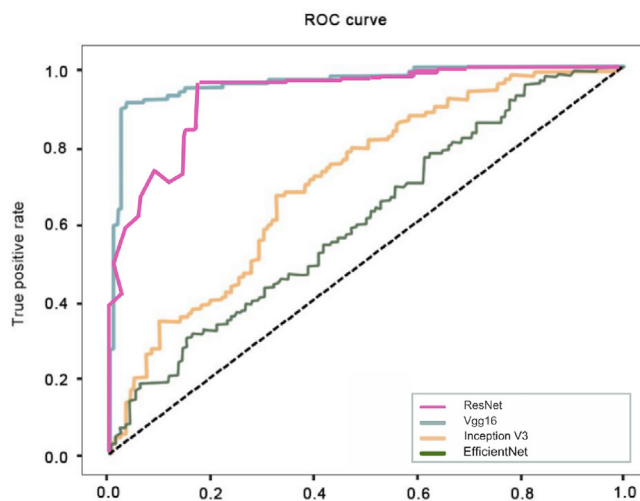


Fig. 13. ROC and AUC curve for cough resemblance.

pre-trained models; VGG-16, InceptionV3, EfficientNet, and ResNet were tested for these two components. Given that, VGG-16 was found to be the most reliable for cough detection with 98% accuracy and ResNet for cough resemblance 93%. The Receiver Operating Characteristic (ROC) curves along with their Area Under the Curve (AUC) for the three models tested for cough resemblance is depicted in Fig. 13. Given that, as explained in Table 9, it was found that a potential COVID-19 patient, either symptomatic or asymptomatic can be detected by analyzing cough sounds with 93% accuracy.

Furthermore, during this study, it was also found that DL using CNNs can have a substantial impact on the automatic detection and extraction of key elements from spectrograms obtained from audio recordings containing coughs, which is relevant to the diagnosis of COVID-19.

Moreover, this study yielded a set of findings about a person's cough and the forced cough sound of a COVID-19 patient. It was revealed that by using CNN and Python libraries for pre-processing, a person's cough can be distinguished from other natural sounds by assessing their frequency fluctuations. It was also discovered that both symptomatic and asymptomatic COVID-19 patients could be identified by analyzing forced cough sounds.

Another fact that was identified in the proposed study is that transfer Learning using the pre-trained model VGG16 showed the maximum accuracy for cough detection while ResNet showed the maximum accuracy for cough resemblance with a limited dataset. On the other hand, it was also found that the confidence of the predictions slightly reduces when there is background noise. However, since the training dataset was crowdsourced, most of these audios contained background noises and were trained accordingly.

Moreover, there is research conducted to analyze cough to detect potential COVID-19 suspects. However, research such as Ismail et al. (2020) attaches a sensor to the front of the neck to get the oscillations to detect cough patterns. In contrast to that study, the proposed system uses a fully contactless approach. Other than that, there are

Table 11
Sub-component accuracies of Shortness of breath detection component.

Process	Accuracy
Capturing breathing pattern	100%
Identifying the nostril area	95%
Detecting inhalation and exhalation	100%
Counting thermal color changes	90%

researches conducted which have developed mobile applications as pre-screening methods by analyzing cough sounds (Laguarta et al., 2020; Imran et al., 2020; Chaudhari et al., 2020; Pal and Sankarasubbu, 2020; Brown et al., 2020; Alsabek et al., 2020; Lella et al., 2021). When reviewing these researches, the majority of them did suggest that asymptomatic patients can be recognized by analyzing cough sounds, which is validated by this study as well.

Some of the limitations found during the study were the limitation and the quality of the dataset; because the dataset used for this is crowd-sourced, there is a risk of the data being mislabeled. Moreover, the dataset collected from the Sri Lankan patients was also of low-quality audio files because the audio were collected through doctors (with the consent of the patients) using a mobile phone. Nonetheless, this component contributes to the possibility of an effective way of identifying COVID-19-positive patients and this will assist to minimize the spread of the disease.

5.1.2. Shortness of breath detection

After following the methodology as mentioned in Section 2, several significant results were obtained for this section. The accuracy of the outcomes of each of the preceding phases is shown in Table 11. As summarized in the table the study can conclude that this component has the capability of identifying a person with shortness of breath with an accuracy of 93%.

Moreover, during this study, it was found that it is possible to obtain the respiratory rate of a person in a contactless approach without affecting a person's privacy. Furthermore, it was found that a person's inhalation and exhalation can be recognized distinctly using thermal footage that captures the person's face. Aside from that, it was discovered that image processing techniques such as thresholding can be utilized to obtain the Region Of Interest of real-time footage. Moreover, it was also found that it is more time efficient to detect this in real-time than using an AI model. In conclusion, it was discovered that a person can be identified as a potential COVID-19 patient by detecting shortness of breath and obtaining the person's respiratory rate using real-time thermal footage.

6. Conclusion and future works

With the spread of the Coronavirus throughout the world, the need for automatic identification of possible COVID-19 suspects arose. As described throughout this paper, this study was able to employ DL together with hardware emulated techniques to identify possible COVID-19 patients using cough classification and shortness of breath without contact with the patient. Both of these components were successfully implemented and yielded an accuracy of 94% for cough classification and 93% for shortness of breath detection using a crowd-sourced dataset and a data set collected from Sri Lankan hospitals. Additionally it was also found that ResNet model was working well with 94% accuracy for early detection of COVID-19 patients in Sri Lankan Context. Moreover, during this study, it was found that COVID patients can be early detected by anosmia, i.e., the inability to smell anything, as a symptom. Even though detecting the anosmia condition was out of scope for this study, during the paper was in review, the authors were able to test anosmia conditions, and the test results showed that promising 97% accuracy in classifying COVID-19 patients during its preliminary stages. Furthermore, the methods developed in

this study hold potential for application beyond COVID-19. The dataset used and the code for the implemented techniques have been published and made available in relevant repositories for further research and utilization. During the study, there were some limitations in the data sets that hindered the accuracy of the models. Particularly, the cleaning process was very challenging because the gathered data sets were crowd-sourced. Hence, there was a risk of the data being mislabeled and such data had to be omitted. Moreover, the low-quality audio files collected from Doctor's mobile phones (with the consent of the patients), was also impacted for accuracy. Such things will be corrected in future implementations. Additionally, a comprehensive dataset from the Sri Lankan Context will be obtained in order to examine correlations between various factors, including gender, age, occupation, etc.

CRedit authorship contribution statement

Rashini Liyanarachchi: Conceptualization, Methodology, Software, Validation, Writing – original draft. **Janaka Wijekoon:** Conceptualization, Supervision, Writing – original draft. **Manujaya Premathilaka:** Conceptualization, Methodology, Software, Validation. **Samitha Vidhanaarachchi:** Writing – original draft.

Declaration of competing interest

The authors declare that they have no known competing financial interests or personal relationships that could have appeared to influence the work reported in this paper.

Data availability

Data will be made available on request

References

- Alkali, A., Saatchi, R., Elphick, H., Burke, D., Evans, R., 2014. Noncontact respiration rate monitoring based on sensing exhaled air. *Malays. J. Fundam. Appl. Sci.* 9, <http://dx.doi.org/10.11113/mjfas.v9n3.97>.
- Alsabek, M.B., Shahin, I., Hassan, A., 2020. Studying the similarity of COVID-19 sounds based on correlation analysis of MFCC. In: 2020 International Conference on Communications, Computing, Cybersecurity, and Informatics (CCCI). pp. 1–5. <http://dx.doi.org/10.1109/CCCI49893.2020.9256700>.
- Apostolopoulos, I., Tzani, B., 2020. Covid-19: Automatic detection from X-Ray images utilizing transfer learning with convolutional neural networks. *Australas. Phys. Eng. Sci. Med. / Support. Australas. Coll. Phys. Sci. Med. Australas. Assoc. Phys. Sci. Med.* 43, <http://dx.doi.org/10.1007/s13246-020-00865-4>.
- Benfante, A., Messina, R., Piccionello, I., Di Liberti, R., Principe, S., Scichilone, N., 2021. The impact of SARS-CoV2 pandemic on the management of IPF patients: Our narrative experience. *Pulm. Pharmacol. Ther.* 69, 102038. <http://dx.doi.org/10.1016/j.pupt.2021.102038>, URL <https://www.sciencedirect.com/science/article/pii/S109455392100050X>.
- Bhattacharya, R., Bandyopadhyay, N., Kalaivani, S., 2017. Real time Android app based respiration rate monitor. In: 2017 International Conference of Electronics, Communication and Aerospace Technology (ICECA), Vol. 1. pp. 709–712. <http://dx.doi.org/10.1109/ICECA.2017.8203633>.
- Botha, G.H.R., Theron, G., Warren, R.M., Klopper, M., Dheda, K., van Helden, P.D., Niesler, T.R., 2018. Detection of tuberculosis by automatic cough sound analysis. *Physiol. Meas.* 39 (4), 045005. <http://dx.doi.org/10.1088/1361-6579/aab6d0>.
- Brown, C., Chauhan, J., Grammenos, A., Han, J., Hasthanasombat, A., Spathis, D., Xia, T., Cicuta, P., Mascolo, C., 2020. Exploring automatic diagnosis of COVID-19 from crowdsourced respiratory sound data. In: Proceedings of the 26th ACM SIGKDD International Conference on Knowledge Discovery and Data Mining. ACM, <http://dx.doi.org/10.1145/3394486.3412865>.
- Chaguzo, C., Coppi, A., Earnest, R., et al., F., 2022. Rapid emergence of SARS-CoV-2 omicron variant is associated with an infection advantage over delta in vaccinated persons. *MedRxiv* <http://dx.doi.org/10.1101/2022.01.22.22269660>, URL <https://www.medrxiv.org/content/early/2022/01/25/2022.01.22.22269660>.
- Chandio, A., Gui, G., Kumar, T., Ullah, I., Ranjbarzadeh, R., Roy, A.M., Hussain, A., Shen, Y., 2022. Precise single-stage detector. <http://dx.doi.org/10.48550/ARXIV.2210.04252>, URL <https://arxiv.org/abs/2210.04252>.
- Chaudhari, G., Jiang, X., Fakhry, A., Han, A., Xiao, J., Shen, S., Khanzada, A., 2020. Virufy: Global applicability of crowdsourced and clinical datasets for AI detection of COVID-19 from cough. <http://dx.doi.org/10.48550/ARXIV.2011.13320>, URL <https://arxiv.org/abs/2011.13320>.
- Covid19.gov.lk, 2021. COVID-19 Sri Lanka update | coronavirus related news Sri Lanka. URL <https://covid19.gov.lk/covid-19-stats.html>.
- Donthu, N., Gustafsson, A., 2020. Effects of COVID-19 on business and research. *J. Bus. Res.* 117, 284–289. <http://dx.doi.org/10.1016/j.jbusres.2020.06.008>, URL <https://www.sciencedirect.com/science/article/pii/S0148296320303830>.
- for Disease Control, C., Prevention, 2021. Coronavirus disease 2019 (COVID-19) – symptoms. URL <https://www.cdc.gov/coronavirus/2019-ncov/symptoms-testing/symptoms.html>.
- 2022a. Github - iisleep/coswara-data: data repository of project coswara.2022. URL <https://github.com/iisleep/Coswara-Data>.
- 2022b. Github - karolpiczak/esc-50: esc-50: dataset for environmental sound classification. URL <https://github.com/karolpiczak/ESC-50>.
- He, K., Zhang, X., Ren, S., Sun, J., 2016. Deep residual learning for image recognition. In: 2016 IEEE Conference on Computer Vision and Pattern Recognition (CVPR). pp. 770–778. <http://dx.doi.org/10.1109/CVPR.2016.90>.
- Imran, A., Posokhova, I., Qureshi, H.N., Masood, U., Riaz, M.S., Ali, K., John, C.N., Hussain, M.I., Nabeel, M., 2020. AI4COVID-19: AI enabled preliminary diagnosis for COVID-19 from cough samples via an app. *Inform. Med. Unlocked* 20, 100378. <http://dx.doi.org/10.1016/j.imu.2020.100378>, URL <https://www.sciencedirect.com/science/article/pii/S2352914820303026>.
- Ismail, M.A., Deshmukh, S., Singh, R., 2020. Detection of COVID-19 through the analysis of vocal fold oscillations. <http://dx.doi.org/10.48550/ARXIV.2010.10707>, URL <https://arxiv.org/abs/2010.10707>.
- Jiang, B., Chen, S., Wang, B., Luo, B., 2022. MGLNN: Semi-supervised learning via multiple graph cooperative learning neural networks. *Neural Netw.* 153, 204–214. <http://dx.doi.org/10.1016/j.neunet.2022.05.024>, URL <https://www.sciencedirect.com/science/article/pii/S0893608022001988>.
- Krug, J.W., Odenbach, R., Boese, A., Friebe, M., 2016. Contactless respiratory monitoring system for magnetic resonance imaging applications using a laser range sensor. *Curr. Dir. Biomed. Eng.* 2 (1), 719–722. <http://dx.doi.org/10.1515/cdbme-2016-0156>.
- Laguarta, J., Hueto, F., Subirana, B., 2020. COVID-19 artificial intelligence diagnosis using only cough recordings. *IEEE Open J. Eng. Med. Biol.* 1, 275–281. <http://dx.doi.org/10.1109/OJEMB.2020.3026928>.
- Larxel, 2021. Covid-19 cough audio classification. URL <https://www.kaggle.com/datasets/andrewmvd/covid19-cough-audio-classification>.
- Le, D.-N., Murugan, V., Gupta, D., Khanna, A., Rodrigues, J., Shankar, D., 2021. IoT enabled depthwise separable convolution neural network with deep support vector machine for COVID-19 diagnosis and classification. *Int. J. Mach. Learn. Cybern.* 12, 1–14. <http://dx.doi.org/10.1007/s13042-020-01248-7>.
- Lella, K.K., PJA, A., 2021. Automatic COVID-19 disease diagnosis using 1D convolutional neural network and augmentation with human respiratory sound based on parameters: cough, breath, and voice. *AIMS Public Health* 8 (2), 240–264. <http://dx.doi.org/10.3934/publichealth.2021019>.
- Liu, Q., Kenny, M., Nilforooshan, R., Barnaghi, P., 2021. An intelligent bed sensor system for non-contact respiratory rate monitoring. <http://dx.doi.org/10.48550/ARXIV.2103.13792>, URL <https://arxiv.org/abs/2103.13792>.
- Liyanarachchi, R., Wijekoon, J., Premathilaka, M., Vidhanaarachchi, S., 2023. COVID-19 cough recording dataset (Sri Lankan). <http://dx.doi.org/10.34740/KAGGLE/DSV/4901461>, URL <https://www.kaggle.com/dsv/4901461>.
- Luis, J.A., Roa Romero, L.M., Gómez-Galán, J.A., Hernández, D.N., Estudillo-Valderrama, M.Á., Barbarov-Rostán, G., Rubia-Marcos, C., 2014. Design and implementation of a smart sensor for respiratory rate monitoring. *Sensors* 14 (2), 3019–3032. <http://dx.doi.org/10.3390/s140203019>, URL <https://www.mdpi.com/1424-8220/14/2/3019>.
- Massaroni, C., Presti, D., Formica, D., Silvestri, S., Schena, E., 2019. Non-contact monitoring of breathing pattern and respiratory rate via RGB signal measurement. *Sensors* 19, 2758. <http://dx.doi.org/10.3390/s19122758>.
- Min, S.D., Kim, J.K., Shin, H.S., Yun, Y.H., Lee, C.K., Lee, M., 2010. Noncontact respiration rate measurement system using an ultrasonic proximity sensor. *IEEE Sens. J.* 10 (11), 1732–1739. <http://dx.doi.org/10.1109/JSEN.2010.2044239>.
- Monge-Álvarez, J., Hoyos-Barceló, C., San-José-Revuelta, L.M., Casaseca-de-la Higuera, P., 2019. A machine hearing system for robust cough detection based on a high-level representation of band-specific audio features. *IEEE Trans. Biomed. Eng.* 66 (8), 2319–2330. <http://dx.doi.org/10.1109/TBME.2018.2888998>.
- Mukhtar, H., Rubaiee, S., Krichen, M., Alrobaea, R., 2021. An IoT framework for screening of COVID-19 using real-time data from wearable sensors. *Int. J. Environ. Res. Public Health* 18 (8), <http://dx.doi.org/10.3390/ijerph18084022>, URL <https://www.mdpi.com/1660-4601/18/8/4022>.
- NA, 2020. Learn about cough. URL <https://www.lung.org/lung-health-diseases/warning-signs-of-lung-disease/cough/learn-about-cough>.
- Nation, U., 2022. Everyone included: social impact of covid-19 | disd_2022. URL <https://www.un.org/development/desa/dspd/everyone-included-covid-19.html>.
- Organization, W.H., 2022a. Coronavirus disease (covid-19): how is it transmitted? 2022. URL <https://www.who.int/news-room/questions-and-answers/item/coronavirus-disease-covid-19-how-is-it-transmitted>.

- Organization, W.H., 2022b. [Link]. URL https://www.who.int/health-topics/coronavirus#tab=tab_1.
- Organization, W.H., 2022c. Tracking sars-cov-2 variants_2022. URL <https://www.who.int/en/activities/tracking-SARS-CoV-2-variants/>.
- Orlandic, L., Teijeiro, T., Atienza, D., 2022. The COUGHVID crowdsourcing dataset: A corpus for the study of large-scale cough analysis algorithms. URL <https://zenodo.org/record/4498364#.YUm8mC0RrRY>.
- Ozturk, T., Talo, M., Yildirim, A., Baloglu, U., Yildirim, Ö., Acharya, U.R., 2020. Automated detection of COVID-19 cases using deep neural networks with X-ray images. *Comput. Biol. Med.* 121, <http://dx.doi.org/10.1016/j.compbiomed.2020.103792>.
- Pal, A., Sankarasubbu, M., 2020. Pay attention to the cough: Early diagnosis of COVID-19 using interpretable symptoms embeddings with cough sound signal processing. <http://dx.doi.org/10.48550/ARXIV.2010.02417>, URL <https://arxiv.org/abs/2010.02417>.
- Panahi, A., Hassanzadeh, A., Moulavi, A., 2020. Design of a low cost, double triangle, piezoelectric sensor for respiratory monitoring applications. *Sens. Bio-Sens. Res.* 30, 9. <http://dx.doi.org/10.1016/j.sbsr.2020.100378>.
- Panwar, H., Gupta, P., Siddiqui, M.K., Morales-Menendez, R., Singh, V., 2020. Application of deep learning for fast detection of COVID-19 in X-Rays using nCOVnet. *Chaos Solitons Fractals* 138, 109944. <http://dx.doi.org/10.1016/j.chaos.2020.109944>.
- Punla, C.S., C. Farro, R., 2022. Are we there yet?: An analysis of the competencies of BEED graduates of BPSU-DC. *Int. Multidiscip. Res. J.* 4 (3), 50–59.
- Quatieri, T.F., Talkar, T., Palmer, J.S., 2020. A framework for biomarkers of COVID-19 based on coordination of speech-production subsystems. *IEEE Open J. Eng. Med. Biol.* 1, 203–206. <http://dx.doi.org/10.1109/OJEMB.2020.2998051>.
- del Rio, C., Collins, L.F., Malani, P., 2020. Long-term health consequences of COVID-19. *JAMA* 324 (17), 1723. <http://dx.doi.org/10.1001/jama.2020.19719>.
- Simonyan, K., Zisserman, A., 2014. Very deep convolutional networks for large-scale image recognition. <http://dx.doi.org/10.48550/ARXIV.1409.1556>, URL <https://arxiv.org/abs/1409.1556>.
- Szegedy, C., Vanhoucke, V., Ioffe, S., Shlens, J., Wojna, Z., 2016. Rethinking the inception architecture for computer vision. In: 2016 IEEE Conference on Computer Vision and Pattern Recognition (CVPR). pp. 2818–2826. <http://dx.doi.org/10.1109/CVPR.2016.308>.
2022. Understanding the mel spectrogram. URL <https://medium.com/analytics-vidhya/understanding-the-mel-spectrogram-fca2afa2ce53>.
- Vaid, S., Kalantar, R., Bhandari, M., 2020. Deep learning COVID-19 detection bias: accuracy through artificial intelligence. *Int. Orthop.* 44, <http://dx.doi.org/10.1007/s00264-020-04609-7>.
- Wang, T., Zhang, D., Wang, L., Zheng, Y., Gu, T., Dorizzi, B., Zhou, X., 2019. Contactless respiration monitoring using ultrasound signal with off-the-shelf audio devices. *IEEE Internet Things J.* 6 (2), 2959–2973. <http://dx.doi.org/10.1109/JIOT.2018.2877607>.
- Yamasinghe, N., Ranasinghe, Y., Dissanayake, Y., Wijekoon, J.L., Panchendrarajan, R., 2022. IMask: An IoT-based intelligent mask to identify and track COVID-19 suspects. In: 2022 IEEE International Conference on Smart Internet of Things (SmartIoT). pp. 7–14. <http://dx.doi.org/10.1109/SmartIoT55134.2022.00011>.